Optimization of Low Dose Metronomic Therapy based on Pharmacological Parameters [1]

Dániel András Drexler * **Levente Kovács** **

* *Physiological Controls Research Center*
Óbuda University
Budapest, Hungary
(email: drexler.daniel@nik.uni-obuda.hu)
** *Physiological Controls Research Center*
Óbuda University
Budapest, Hungary
(email: kovacs.levente@nik.uni-obuda.hu)

Abstract: Therapeutic optimization is a promising direction of computer aided medicine. Optimization of chemotherapy based on mathematical models can result in lower doses, fewer side effects, a smaller chance of acquired drug resistance and more efficient personification. We explore model-based chemotherapy optimization for high frequency low dose therapies with impulsive inputs. We keep the drug level over a specified value using the minimal value of injection doses. We generate therapy for population mean parameters acquired from identification based on mice experiments. We carry out in silico trials based on the results of the individual fits from the identification process and test the therapy generated for the population mean parameters. The results show that therapy optimization based on population mean parameters can be used to generate therapy for the individuals and results in a solution close to the optimal one without using specific knowledge about the individual.

Keywords: chemotherapy optimization, biomedical control, impulsive control, positive system, compartment system

1. INTRODUCTION

Conventional chemotherapy protocols use large doses of drugs with large resting time (i.e., the time between the injections), see e.g., Pérez-García et al. (2019). A typical approach is to use Maximal Tolerable Dose (MTD) of the drug in hope of achieving maximal effect. On the contrary, Low-Dose Metronomic chemotherapy (LDM) uses low dose high density drug administration versus MTD treatment, which was proven more effective e.g., against cancer cells that tend to become resistant against the drug (Browder et al. (2000)). Besides coping with resistance, LDM therapy may also be cheaper and have less side effects. However, scheduling the therapy is challenging. An alternative to solve this problem is to create a mathematical model of the tumor dynamics describing the effect of the drug (Akhmetzhanov et al. (2019); Greene et al. (2019); Pérez-García et al. (2019); Smalley et al. (2019)) and generate the optimal therapy based on the model like in Cacace et al. (2020); Drexler and Kovács (2019); Drexler et al. (2017b); Pérez-García et al. (2019).

The mathematical model of tumor dynamics is a fundamental component of model-based optimization. There are numerous tumor models in the literature, see e.g., the works of Altrock et al. (2015); Jarrett et al. (2018); Lowengrub et al. (2010); here we focus on models described by ordinary differential equations, since they are more suitable to describe population mean characteristics and their handling in optimization and control is easier compared to partial differential equations and other alternatives.

We use a fourth-order model created to describe measurements from animal experiments first for angiogenic therapy using bevacizumab (Drexler et al. (2017a); Sápi et al. (2015)), and later for chemotherapy using pegylated liposomal doxorubicin (PLD) in Drexler et al. (2020) based on the experiments from Füredi et al. (2017), discussed in Section 2. The latest model has four states variables, two state variables for the living and dead tumor volume dynamics and two state variables to describe the pharmacokinetics of the drug as a two compartment model.

[1] This project has received funding from the European Research Council (ERC) under the European Union's Horizon 2020 research and innovation programme (grant agreement No 679681). Project no. 2019-1.3.1-KK-2019-00007. has been implemented with the support provided from the National Research, Development and Innovation Fund of Hungary, financed under the 2019-1.3.1-KK funding scheme. This research was also supported by the Eötvös Loránd Research Network Secretariat under grant agreement no. ELKH KÖ-40/2020 ('Development of cyber-medical systems based on AI and hybrid cloud methods'). This research was supported partially by Horizon2020-2017-RISE-777911 project. The present work has also been supported by the Hungarian National Research, Development and Innovation Office (2018-2.1.11-TÉT-SI-2018-00007 and SNN 125739).

We formulate the optimization problem as maintaining a predefined drug level during the therapy with the low amount of injections, i.e., we carry out optimal impulsive control of the two compartment pharmacokinetic model.

Optimal impulsive control of compartment systems has long been engaged in the scientific community, see e.g., Pierce and Schumitzky (1976). The optimal solution for keeping the drug level over a specified dose was given by Kusuoka et al. (1981), which we briefly summarize in Subsection 3.1. They also showed that if the time between the injections is large enough, then the optimal therapy consists of a larger dose at the beginning followed by smaller doses with the same value for a compartment model defining oral administration of a drug. We show in Subsection 3.2 that this characteristics holds for two compartment models if their dynamics and the resting time satisfy certain conditions.

The optimal drug administration is tested in silico in Section 4 with the tumor growth model given in Section 2 describing the effect of cytotoxic drug PLD discussed in Drexler et al. (2020, 2019) applied for mice experiments from Füredi et al. (2017). The robustness is tested by generating the optimal therapy for the population mean parameters in Subsection 4.1 and testing the generated therapy for the individual fits in Subsection 4.2. The results show that the generated therapy is effective on all the individuals, which may indicate that personification of the therapy may not require determining the specific model parameters related to a patient; it is enough if we know the mean parameters of a well specified group the patient belongs to.

2. TUMOR GROWTH MODEL FOR CHEMOTHERAPY

2.1 Tumor dynamics

We use a fourth-order model to describe tumor dynamics, pharmacodynamics and pharmacokinetics as

$$\dot{x}_1 = (a-n)\,x_1 - b\frac{x_1 x_3}{ED_{50}+x_3} \tag{1}$$

$$\dot{x}_2 = nx_1 + b\frac{x_1 x_3}{ED_{50}+x_3} - wx_2 \tag{2}$$

$$\dot{x}_3 = -(c+k_1)\,x_3 + k_2 x_4 - b_k\frac{x_1 x_3}{ED_{50}+x_3} \tag{3}$$

$$\dot{x}_4 = k_1 x_3 - k_2 x_4 \tag{4}$$

where x_1, x_2, x_3 and x_4 are the time functions of the living tumor volume, dead tumor volume, drug level in the central compartment and drug level in the peripherial compartment, respectively. The volumes are given in mm^3, while the drug levels are in mg/kg. The injections are modeled as impulsive effects on the central compartment x_3. The output of the system is the total tumor volume

$$y = x_1 + x_2. \tag{5}$$

The model parameters have been identified in Drexler et al. (2020) using mice experiments from Füredi et al. (2017). The identified parameters for the population mean are shown in Table 1, while the identified parameter values for the individuals (labeled as PLD2, PLD3, PLD4, PLD5, PLD6, PLD9 and PLD10 in Füredi et al. (2017)) are shown in Table 2. Note that the identification showed that the value of b_k is negligible, thus we use $b_k = 0$ throughout the paper and the parameter b_k is not contained in the Tables.

2.2 Pharmacodynamic model

The pharmacodynamics of the drug is defined by the Hill function $x_3/(ED_{50}+x_3)$ in the equations (1)-(3). This function expresses that the effect of the drug is saturated, thus after a given limit, increasing the drug level yields a very low increase in the drug effect. The effective median dose parameter ED_{50} is the drug concentration where the effect is 50%, i.e., the value of the Hill function is 0.5.

The pharmacodynamics characterizes the desired value of the drug level in the central compartment that should be maintained by the therapy discussed in Section 3. One of the constraints of the therapy optimization will be to keep the drug level on the central compartment over a certain limit m. Due to the pharmacodynamics, this limit will be specified as a constant multiple of the ED_{50} parameter, i.e., $m = \kappa ED_{50}$. If κ is sufficiently large, the value of the Hill function is close to 1, i.e., close to the maximal effect of the drug. We will use $\kappa = 100$ in the in silico tests in Section 4.

2.3 Pharmacokinetic model

The pharmacokinetics of the model is described by (3)-(4), which is a linear time-invariant system if $b_k = 0$. The input of the system is impulsive and has effect on x_3. In the pharmacodynamics model described by the Hill function in the last term of the right-hand side of (1), x_3 has effect on the tumor, thus the output y_p of the pharmacokinetic model is x_3. Thus, the differential equation of the pharmacokinetic model is

$$\begin{pmatrix}\dot{x}_3\\ \dot{x}_4\end{pmatrix} = \underbrace{\begin{pmatrix}-c-k_1 & k_2\\ k_1 & -k_2\end{pmatrix}}_{\boldsymbol{A}}\begin{pmatrix}x_3\\ x_4\end{pmatrix} + \begin{pmatrix}1\\ 0\end{pmatrix}u \tag{6}$$

with u being the sum of impulsive inputs, i.e.,

$$u(t) = \sum_{k=0}^{K-1} u_k \delta(t-t_k), \tag{7}$$

at $t \geq 0$, where K is the total number of injections, t_k, $k = 0, 1, \ldots, K-1$ is the time of injections with doses u_k, $k = 0, 1, \ldots, K-1$, and δ is the Dirac delta distribution.

The response of the pharmacokinetic subsystem (6) with output x_3 for inputs (7) at time t can be written as the sum of impulse responses of the system as

$$y_p(t) = \sum_{k=0}^{K-1} w(t-t_k)u_k. \tag{8}$$

The impulse response of the pharmacokinetic subsystem is

$$w(t) = \frac{\lambda_1+k_2}{\lambda_1-\lambda_2}e^{\lambda_1 t} + \frac{\lambda_2+k_2}{\lambda_2-\lambda_1}e^{\lambda_2 t}, \tag{9}$$

where λ_1 and λ_2 are the eigenvalues of the system matrix $\boldsymbol{A}$ in (6) and can be expressed with the parameters as

$$\lambda_{1,2} = \frac{-(c+k_1+k_2) \pm \sqrt{(c+k_1+k_2)^2 - 4ck_2}}{2}. \tag{10}$$

Parameter	Est.	SE	%RSE	Back-transformed (95 %CI)	BSV (CV%)
Log a	-2.08	0.207	9.94	0.125 (0.0834, 0.187)	47.6
Log n	-8.07	4.81	59.5	0.000312 ($2.53{\cdot}10^{-8}$, 3.85)	178.
Log b	-0.801	0.296	37	0.449 (0.251, 0.802)	59.9
Log ED50	-7.48	3.18	42.5	0.000562 ($1.11{\cdot}10^{-6}$, 0.285)	2480.
Log w	-3.29	0.42	12.7	0.0371 (0.0163, 0.0845)	143.
Log c	-0.211	0.216	103	0.81 (0.53, 1.24)	36.2
Log k1	1.91	1.31	68.6	6.78 (0.518, 88.8)	82.0
Log k2	4.2	0.971	23.1	66.7 (9.95, 447)	113.
Additive error	109			109	

Table 1. The estimated population mean parameter values for the model. (SE: standard error, RSE: relative standard error, BSV: between-subject variation, CI: confidence interval, CV: coefficient of variation.)

	PLD2	PLD3	PLD4	PLD5	PLD6	PLD9	PLD10
a	0.1104	0.2155	0.1677	0.1409	0.1466	0.1005	0.06409
b	0.4201	0.4712	0.77	0.414	0.3977	0.6388	0.2283
c	0.9204	0.7113	1.124	0.5919	0.6352	0.7456	1.217
ED_{50}	0.00148	$5.03 \cdot 10^{-5}$	$8.96 \cdot 10^{-5}$	0.0007299	0.001534	0.001392	0.0003237
k_1	7.182	10.37	4.665	5.139	10.03	7.428	5.456
k_2	74.43	34.27	69.09	139.9	62.82	69.76	60.57
n	0.0002683	0.0002695	0.0003212	0.0002778	0.0002762	0.0003446	0.0002824
w	0.01534	0.08779	0.06445	0.01481	0.0874	0.01193	0.0978

Table 2. The estimated parameter values for the individual fits

The pharmacokinetic subsystem is kinetic, thus it is positive (Érdi and Tóth (1989); Tóth et al. (2018); Vol'pert (1972)), which implies that the impulse response of the system is also positive for all $t \geq 0$.

Lemma 1. The pharmacological subsystem is asymptotically stable and non-oscillatory.

Proof. Asymptotic stability is a consequence of the compartmental system (Tóth et al. (2018)), and non-oscillatory behaviour is the consequence of the positivity of the planar system □

Let λ_1 be the eigenvalue with the larger absolute value, thus we can write $\lambda_1 = \beta\lambda_2$ with $\beta > 1$. Using this notation, the impulse response (9) can be reformulated to

$$w(t) = e^{\lambda_2 t}\frac{\lambda_2 e^{\lambda_2(\beta-1)t}\left(\lambda_2\beta + k_2\right) - \left(\lambda_2 + k_2\right)}{\lambda_2(\beta-1)}. \quad (11)$$

In general, for a second-order compartment model, the impulse response is

$$w(t) = c_1 e^{\lambda_1 t} + c_2 e^{\lambda_2 t}, \quad (12)$$

which can be reformulated as

$$w(t) = e^{\lambda_2 t}\left(c_1 e^{\lambda_2(\beta-1)t} + c_2\right). \quad (13)$$

Assumption 1. We assume that β and t is large enough so that $e^{\lambda_2(\beta-1)t} \approx 0$.

Using the population mean parameters in Table 1, the eigenvalues of the pharmacokinetic subsystem's system matrix are

$$\lambda_1 = -73.55 \quad (14)$$
$$\lambda_2 = -0.7345, \quad (15)$$

thus $\beta = 100.13$, and $e^{\lambda_2(\beta-1)t} = 2.37 \cdot 10^{-32}$ for $t = 1$ day, which can be considered as zero. In what follows, we suppose that Assumption 1 holds and consider the term $\exp(\lambda_2(\beta-1)t)$ as zero.

Lemma 2. Suppose that Assumption 1 holds, and let $t_2 > t_1 > 0$, then

$$\frac{w(t_2)}{w(t_1)} \approx e^{(t_2-t_1)\lambda_2}. \quad (16)$$

Proof. Using (11) and Assumption 1, we can write the ratio of the impulse responses as

$$\frac{w(t_2)}{w(t_1)} = \frac{e^{\lambda_2 t_2}\left(c_1 e^{\lambda_2(\beta-1)t_2} + c_2\right)}{e^{\lambda_2 t_1}\left(c_1 e^{\lambda_2(\beta-1)t_1} + c_2\right)} \quad (17)$$
$$\approx \frac{e^{\lambda_2 t_2} c_2}{e^{\lambda_2 t_1} c_2} = \frac{e^{\lambda_2 t_2}}{e^{\lambda_2 t_1}} = e^{\lambda_2(t_2-t_1)}. \quad (18)$$

□

Note that we will use equality in (16) later in the paper.

3. OPTIMAL IMPULSIVE THERAPY

We are looking for the optimal injection doses u_k given at times instants t_k, $k = 0, 1, \ldots, K-1$, such that the level of the drug in the central compartment is large enough all the time to have sufficiently large effect. This problem has been addressed by Kusuoka et al. (1981), who formulated and solved this optimization problem for compartmental systems. We review their result in Subsection 3.1 and apply them for our pharmacokinetic model and for the special case of fix time between injections and two compartment models in Subsection 3.2.

3.1 Optimal drug doses for compartment models

Let $\boldsymbol{u} = (u_0, u_2, \ldots, u_{K-1})^\top$ and $\mathbf{1} = (1, 1, \ldots, 1)^\top$ be a column vector with elements of one and length K, and let $\boldsymbol{\Phi}$ be the matrix of impulse responses constructed as

$$\boldsymbol{\Phi} = \{w(t_i - t_{j-1})\}_{i,j} \quad (19)$$

where $i, j = 1, 2, \ldots, K$, and t_K is a time instant after the last injection, i.e., $t_K > t_{K-1}$.

The goal is to have $w(t) \geq m$ for all $t \geq 0$, where m is the desired lower limit for the drug level, while having positive injections and minimizing the total amount of injections. Since the system is asymptotically stable and non-oscillating, $w(t) \geq m$ for all $t \geq 0$ is equivalent to $w(t_k) \geq m$ for all t_k, $k = 0, 1, \ldots, K$. Thus, the optimization problem can be written as

$$\begin{aligned} &\min \mathbf{1}^\top \boldsymbol{u} \\ &\text{subject to} \\ &\boldsymbol{\Phi u} \geq m\mathbf{1}, \quad \boldsymbol{u} \geq 0. \end{aligned} \tag{20}$$

The solution to this optimization problem was given in Kusuoka et al. (1981) as

$$\tilde{\boldsymbol{u}} = m\boldsymbol{\Phi}^{-1}\mathbf{1}. \tag{21}$$

3.2 Optimal injection doses with fixed resting time

Let the time between the injections be fix and denote it by T_s. Then, $t_i - t_j = (i-j)T_s$, for all $i > j$ and $i = 1, \ldots, K$ (note that there is no injection at t_K, it is the terminal time of the therapy) and $j = 0, 1, \ldots, K-1$. Thus, the matrix of impulse responses can be written as

$$\boldsymbol{\Phi} = \begin{pmatrix} w(T_s) & 0 & \ldots & 0 \\ w(2T_s) & w(T_s) & \ldots & 0 \\ \vdots & \vdots & \ddots & \vdots \\ w(KT_s) & w((K-1)T_s) & \ldots & w(T_s) \end{pmatrix} \tag{22}$$

which is a lower triangular Toeplitz matrix.

Lemma 3. Suppose that Assumption 1 holds. The inverse of $\boldsymbol{\Phi}$ given in (22) with fixed time between injections is a lower triangular Toeplitz matrix with first column as

$$\boldsymbol{v} = (v_1, v_2, 0, \ldots, 0)^\top \tag{23}$$

with $v_1 = 1/w(T_s)$ and $v_2 = -1/w(T_s)e^{\lambda_2 T_s}$.

Proof. The inverse of a lower triangular Toeplitz matrix is a lower triangular Toeplitz matrix whose elements can be calculated recursively as shown in Trench (2009). Let the first column of $\boldsymbol{\Phi}$ be $\boldsymbol{w} = (w_1, w_2, \ldots, w_K)^\top$ with $w_k := w(kT_s)$ and the first column of the inverse matrix be denoted by $\boldsymbol{v} = (v_1, v_2, \ldots, v_K)^\top$. Then, the elements of the inverse matrix can be calculated recursively as

$$v_k = -\frac{1}{w_1}\sum_{n=1}^{k-1} v_n w_{k-n+1}, \tag{24}$$

for $k > 1$ and $v_1 = 1/w_1$. Thus, for $k = 2$ we have

$$v_2 = -\frac{1}{w_1}v_1 w_2 = -\frac{1}{w_1}\frac{w_2}{w_1} = -\frac{1}{w_1}\Delta \tag{25}$$

with $\Delta = w_2/w_1$. For $k = 3$, we get

$$\begin{aligned} v_3 &= -\frac{1}{w_1}(v_1 w_3 + v_2 w_2) = -\frac{v_1 w_3}{w_1} - \frac{v_2 w_2}{w_1} \\ &= -\frac{v_1 w_3}{w_2}\frac{w_2}{w_1} - \frac{v_2 w_2}{w_1} = -v_1\Delta^2 - v_2\Delta \\ &= -\frac{1}{w_1}\Delta^2 - \left(-\frac{1}{w_1}\Delta\right)\Delta = 0 \end{aligned} \tag{26}$$

where we have used that $\Delta = w_2/w_1 = w_3/w_2 = e^{T_s\lambda_2}$ due to Lemma 2. Similarly, $\Delta = w_k/w_{k-1}$ for all $k = 2, \ldots, K$, and $w_i/w_j = \Delta^{i-j}$ for $i > j$, $i = 2, 3, \ldots, K$ and $j = 1, 2, \ldots, K-1$. Generally, for $k > 2$, we have that

$$\begin{aligned} v_k &= -\frac{1}{w_1}(v_1 w_k + v_2 w_{k-1} + \ldots v_{k-1} w_2) \\ &= -\left(v_1\Delta^{k-1} + v_2\Delta^{k-2} + \ldots v_{k-1}\Delta\right) \end{aligned} \tag{27}$$

and for $k+1$, we get

$$\begin{aligned} v_{k+1} &= -\left(v_1\Delta^k + v_2\Delta^{k-1} + \ldots v_{k-1}\Delta^2 + v_k\Delta\right) \\ &= -\Delta\left(v_1\Delta^{k-1} + v_2\Delta^{k-2} + \ldots v_{k-1}\Delta + v_k\right) \\ &= -\Delta\left(v_1\Delta^{k-1} + v_2\Delta^{k-2} + \ldots v_{k-1}\Delta\right) - \Delta v_k \\ &= \Delta v_k - \Delta v_k = 0, \end{aligned} \tag{28}$$

which implies that $v_k = 0$ for all $k \geq 3$. Thus, the inverse matrix is a lower triangular Toeplitz matrix with the first element of its first column being $1/w_1 = 1/w(T_s)$, the second element of its first column being $-1/w_1\Delta = -1/w(T_s)\exp(\lambda_2 T_s)$ and the remaining elements of the first column are zero. □

Theorem 4. Suppose that Assumption 1 holds. Then the minimal injection doses that are required to keep the drug level over a limit m are $\tilde{u}_0 = m/w(T_s)$ and $\tilde{u}_k = m/w(T_s)(1 - \exp(T_s\lambda_2))$ for $k = 1, 2, \ldots, K-1$.

Proof. Substitute the result of Lemma 3 into (21). □

This result has been shown by Kusuoka et al. (1981) using different derivation for a specific two compartment system describing the pharmacokinetics of oral drug administration. We showed here that this is true for general two compartment models if Assumption 1 holds. Moreover, this result can be generalized for any compartments if they have a dominant eigenvalue and the resting time is sufficiently large. Note that a condition for (21) to be optimal is that the resting time is larger than the time when the impulse response of the system reaches its maximum (and due to nonoscillatory behaviour, there is only one such time) as it was shown by Kusuoka et al. (1981). Assumption 1 also implies that this condition is satisfied.

4. IN SILICO ROBUSTNESS ANALYSIS

4.1 Therapy generation for the population mean

First, we carried out in silico test of the optimal input generation algorithm for the population mean parameters provided in Table 1 with rest period of $T_s = 1$ day and 30 days of therapy. Initially, the living tumor volume was considered to be 200 mm^3, while all the other variables were initially zero.

The generated injection doses are shown by the green dots in the lower figure of Fig. 1, while the drug level in the central compartment is shown by the blue solid curve in the lower figure. The upper figure of Fig. 1 shows the effect of the therapy on the living (green curve), dead (red curve) and total tumor volumes (blue curve). The results show that the therapy is effective in the 30 days since the living tumor cells are eliminated after about 11 days. After this time, the total tumor volume is almost entirely consisted of the dead tumor cells.

4.2 Effect of the generated therapy on the individuals

Next, we used the therapy generated for the population mean parameters in Subsection 4.1 and applied it in silico

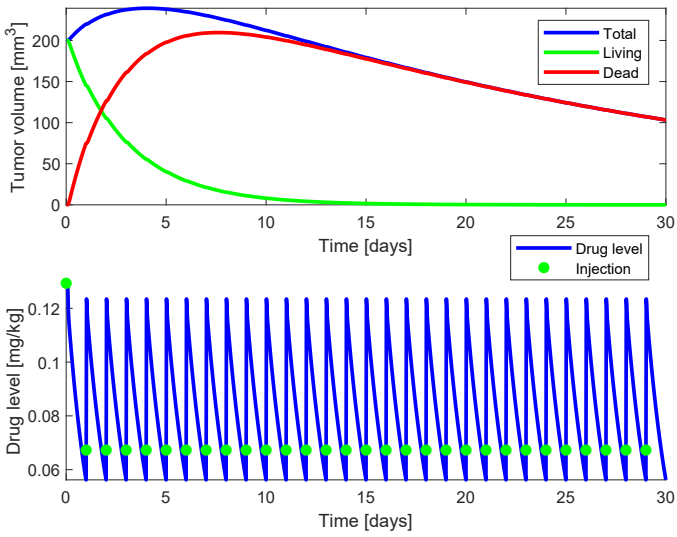

Fig. 1. The optimal therapy generated for the population mean parameters and tested in silico with the population mean parameters

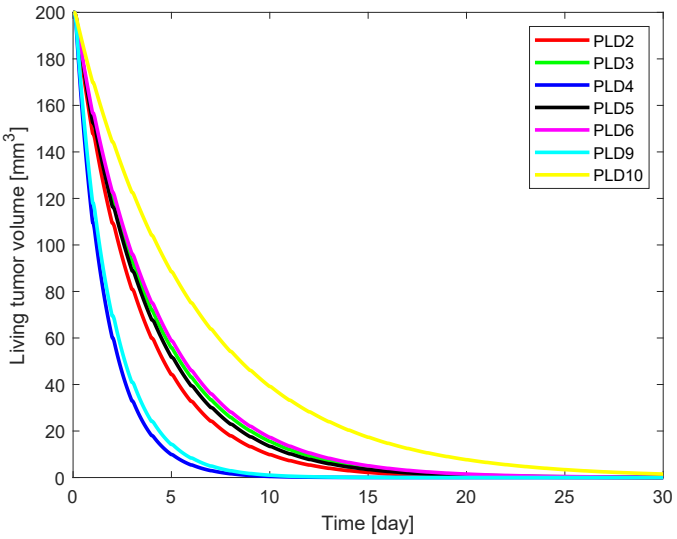

Fig. 2. The living tumor volumes (x_1) with the optimal therapy generated for the population mean parameters and tested in silico with the individual fits

for the individual fits with parameters given in Table 2. The resting time was chosen as 1 day and the final time as 30 days, the same way as in Subsection 4.1. Also, the initial value of the living tumor volume was considered to be 200 mm^3, while all the other variables were initially set to zero.

Figure 2 shows the regression of the living tumor volumes. These curves show an exponential behaviour, since these are the solutions of the differential equation (1), which can be approximated as

$$\dot{x}_1 \geq \left(a - n - b \frac{x_{3,min}}{ED50 + x_{3,min}} \right) x_1, \qquad (29)$$

and since the derivative of the Hill function $x_3/(ED_{50}+x_3)$ is small for $x_3 >> ED_{50}$ which holds for $x_{3,min}$ due to the constraints of the therapy, the dynamics of the living tumor volume is close to linear, and can be well approximated by an exponential curve.

For comparison of the effect of the therapy on the individuals, we have determined a regression time constant T_{reg} for all the in silico results by constructing the tangent lines at zero for all the living tumor volume curves and calculating the intersection of these lines with the time axis. The time constants are shown in Table 3 in ascending order along with the corresponding b and ED_{50} parameters of the individuals. The results show that the regression time is in close relation with the parameter b which characterizes the effect of the drug, since the parameter b decreases as T_{reg} increases. The only exception for this is for PLD3, which has a much larger tumor growth rate parameter a than the other individuals which is 72.5% larger than the population mean (see Table 2). The last row of Table 3 shows the derived value of $a-n-bx_{3,min}/(ED_{50}+x_{3,min})$ for each individual, which is the rate of the approximating differential equation (29) and truly characterizes the speed of regression.

5. CONCLUSION

The minimal injection doses to keep the drug level in the central compartment above a specified limit (100 times the effective median dose) were calculated for the virtual mice with mean value parameters, and the generated therapy was tested in silico with the parameter sets describing the real mice acquired from parametric identification based on experiments. The in silico trials prove that therapy generation can be done based on pharmacological parameters, while the parameters specific to tumor dynamics only describe the final outcome resulted from the therapy, and have no effect on the required input, apart from the length of the therapy.

Furthermore, the in silico trials showed that if we can cluster patients based on the tumor model parameters and can specify mean value parameters for the given clusters, then the therapy can be generated for the mean values and will result in a therapy close to optimal for all the patients in the cluster.

REFERENCES

Akhmetzhanov, A.R., Kim, J.W., Sullivan, R., Beckman, R.A., Tamayo, P., and Yeang, C.H. (2019). Modelling bistable tumour population dynamics to design effective treatment strategies. *Journal of theoretical biology*, 474, 88–102.

Altrock, P.M., Liu, L.L., and Michor, F. (2015). The mathematics of cancer: integrating quantitative models. *Nature Reviews. Cancer*, 15(12), 730–745. doi: 10.1038/nrc4029.

Browder, T., Butterfield, C.E., Kra¨ling, B.M., Shi, B., Marshall, B., O'Reilly, M.S., and Folkman, J. (2000). Antiangiogenic scheduling of chemotherapy improves efficacy against experimental drug-resistant cancer. *Cancer Research*, 60, 1878–1886.

Cacace, F., Cusimano, V., and Palumbo, P. (2020). Optimal impulsive control with application to antiangiogenic tumor therapy. *IEEE Transactions on*

	PLD4	PLD9	PLD2	PLD5	PLD3	PLD6	PLD10
T_{reg} [day]	2.074	2.329	3.86	4.381	4.402	4.672	6.791
b [1/day]	0.77	0.6388	0.4201	0.414	0.4712	0.3977	0.2283
ED_{50} [mg/kg]	$8.96{\cdot}10^{\ 5}$	0.001392	0.00148	0.0007299	$5.03{\cdot}10^{\ 5}$	0.001534	0.0003237
$a-n-\gamma b$ [1/day]	-0.6011	-0.5235	-0.2923	-0.2692	-0.2556	-0.2413	-0.1621

Table 3. The regression time constants of the living tumor volumes as the effect of the therapy in ascending order, and the corresponding b and ED_{50} parameters and the derived $a-n-\gamma b$ with parameters of the individuals with $\gamma = x_{3,min}/(ED_{50}+x_{3,min})$.

Control Systems Technology, 28(1), 106–117. doi: 10.1109/TCST.2018.2861410.

Drexler, D.A. and Kovács, L. (2019). Optimization of impulsive discrete-time tumor chemotherapy. In *Proceedings of the 2019 IEEE 1st International Conference on Societal Automation.*

Drexler, D.A., Sápi, J., and Kovács, L. (2017a). Modeling of tumor growth incorporating the effects of necrosis and the effect of bevacizumab. *Complexity*, 1–11. doi: 10.1155/2017/5985031.

Drexler, D.A., Sápi, J., and Kovács, L. (2017b). Optimal discrete time control of antiangiogenic tumor therapy. *IFAC-PapersOnLine*, 50(1), 13504 – 13509. doi:https://doi.org/10.1016/j.ifacol.2017.08.2337. 20th IFAC World Congress.

Drexler, D.A., Ferenci, T., Füredi, A., Szakács, G., and Kovács, L. (2020). Experimental data-driven tumor modeling for chemotherapy. *IFAC-PapersOnLine*, 53(2), 16245–16250. doi: https://doi.org/10.1016/j.ifacol.2020.12.619. 21th IFAC World Congress.

Drexler, D.A., Ferenci, T., Lovrics, A., and Kovács, L. (2019). Tumor dynamics modeling based on formal reaction kinetics. *Acta Polytechnica Hungarica*, 16, 31–44. doi:10.12700/APH.16.10.2019.10.3.

Érdi, P. and Tóth, J. (1989). *Mathematical Models of Chemical Reactions. Theory and Applications of Deterministic and Stochastic Models.* Princeton University Press, Princeton, New Jersey.

Füredi, A., Szebényi, K., Tóth, S., Cserepes, M., Hámori, L., Nagy, V., Karai, E., Vajdovich, P., Imre, T., Szabó, P., Szüts, D., Tóvári, J., and Szakács, G. (2017). Pegylated liposomal formulation of doxorubicin overcomes drug resistance in a genetically engineered mouse model of breast cancer. *Journal of Controlled Release*, 261, 287–296. doi:10.1016/j.jconrel.2017.07.010.

Greene, J.M., Gevertz, J.L., and Sontag, E.D. (2019). Mathematical approach to differentiate spontaneous and induced evolution to drug resistance during cancer treatment. *JCO Clinical Cancer Informatics*, (3), 1–20. doi:10.1200/CCI.18.00087.

Jarrett, A.M., Lima, E.A.B.F., Hormuth, D.A., McKenna, M.T., Feng, X., Ekrut, D.A., Resende, A.C.M., Brock, A., and Yankeelov, T.E. (2018). Mathematical models of tumor cell proliferation: A review of the literature. *Expert Review of Anticancer Therapy*, 18(12), 1271–1286. doi:10.1080/14737140.2018.1527689.

Kusuoka, H., Kodama, S., Maeda, H., Inoue, M., Hori, M., Abe, H., and Kajiya, F. (1981). Optimal control in compartmental systems and its application to drug administration. *Mathematical Biosciences*, 53(1), 59–77. doi:10.1016/0025-5564(81)90039-0.

Lowengrub, J.S., Frieboes, H.B., Jin, F., Chuang, Y.L., Li, X., Macklin, P., Wise, S.M., and Cristini, V. (2010). Nonlinear modelling of cancer: bridging the gap between cells and tumours. *Nonlinearity*, 23(1), R1–R9. doi: 10.1088/0951-7715/23/1/r01.

Pérez-García, V.M., Ayala-Hernández, L.E., Belmonte-Beitia, J., Schucht, P., Murek, M., Raabe, A., and Sepúlveda, J. (2019). Computational design of improved standardized chemotherapy protocols for grade ii oligodendrogliomas. *PLoS Computational Biology*, 15(7). E1006778.

Pierce, J.G. and Schumitzky, A. (1976). Optimal impulsive control of compartment models, I: Qualitative aspects. *Journal of Optimization Theory and Applications*, 18(4), 537–554. doi:10.1007/BF00932661. URL `https://doi.org/10.1007/BF00932661`.

Sápi, J., Kovács, L., Drexler, D.A., Kocsis, P., Gajári, D., and Sápi, Z. (2015). Tumor volume estimation and quasi-continuous administration for most effective bevacizumab therapy. *PLoS ONE*, 10(11), 1–20. doi: 10.1371/journal.pone.0142190.

Smalley, I., Kim, E., Li, J., Spence, P., Wyatt, C.J., Eroglu, Z., Sondak, V.K., Messina, J.L., Babacan, N.A., Maria-Engler, S.S., Armas, L.D., Williams, S.L., Gatenby, R.A., Chen, Y.A., Anderson, A.R.A., and Smalley, K.S.M. (2019). Leveraging transcriptional dynamics to improve BRAF inhibitor responses in melanoma. *EBioMedicine*, 48, 178 – 190. doi: https://doi.org/10.1016/j.ebiom.2019.09.023.

Tóth, J., Nagy, A.L., and Papp, D. (2018). *Reaction kinetics: exercises, programs and theorems.* Springer.

Trench, W.F. (2009). Inverses of lower triangular Toeplitz matrices. URL `http://works.bepress.com/william_trench/132/`.

Vol'pert, A.I. (1972). Differential equations on graphs (in Russian). *Mathematics of the USSR-Sbornik*, 17(4), 571.